PREDICTING THE ONSET OF CAVITATION IN AUTOMOTIVE TORQUE CONVERTERS: PART I – DESIGNS WITH GEOMETRIC SIMILITUDE

D. L. Robinette, J. M. Schweitzer and D. G. Maddock
General Motors Powertrain Group
General Motors Corporation

C. L. Anderson, J. R. Blough and M. A. Johnson
Michigan Technological University
Dep't of Mechanical Engineering – Engineering Mechanics

ABSTRACT

Dimensional analysis has been applied to automotive torque converters to understand the response of performance to changes in torque, size, working fluid or operating temperature. The objective of this investigation was to develop a suitable dimensional analysis for estimating the effect of exact geometric scaling of a particular torque converter design on the onset of cavitation. Torque converter operating thresholds for cavitation were determined experimentally with a dynamometer test cell at the stall operating condition using nearfield acoustical measurements. Dimensionless quantities based upon either speed or torque at the onset of cavitation and flow properties (e.g. pressures and temperature dependent fluid properties) were developed and compared. The proposed dimensionless stator torque quantity was found to be the most appropriate scaling law for extrapolating cavitation thresholds to multiple diameters. A power product model was fit on dimensionless stator torque data to create a model capable of predicting cavitation thresholds. Comparison of the model to test data taken over a range of operating points showed an error of 3.7%. This is the first paper of a two part paper. In Part II, application of dimensional analysis will be expanded from torque converters with exact geometric similitude to those of more general design.

INTRODUCTION

The automotive torque converter is the powertrain component that transfers power from the engine to the gear system of the automatic transmission. It multiplies torque at low speed to overcome the poor low speed torque characteristics of an internal combustion engine. Torque converters are classified as a turbomachine as most modern designs typically contain multi-bladed elements, including a mixed flow pump and turbine and an axial flow stator. A typical cross section diagram of a three element converter and closed loop toroidal flow path are shown in Figure 1. The flow is highly three dimensional with secondary flow structures as a result of the close proximity of each element and the closed loop flow. Torque converters produce maximum torque multiplication at low speed ratio and high efficiency at high speed ratio. Speed ratio is defined as the rotation of turbine speed divided by pump speed.

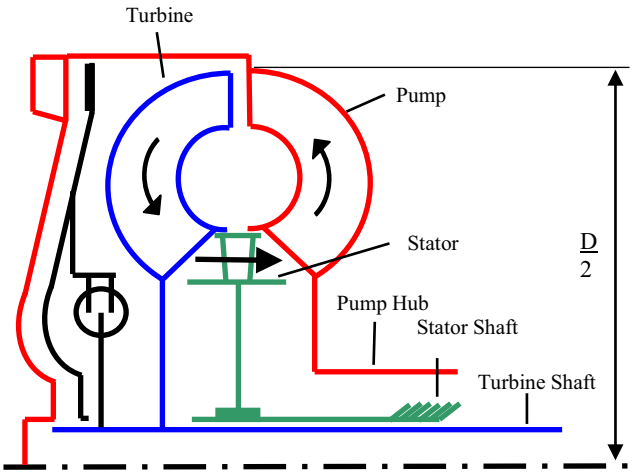

Figure 1. Cross section schematic of a modern three element torque converter, arrows indicate direction of toroidal flow.

The pump rotates at engine speed and torque, imparting an increase in angular momentum on the fluid from inner to outer radius of the torus, guiding the fluid into the turbine. The turbine extracts angular momentum from the fluid, transmitting a torque to the automatic transmission via the turbine shaft. The fluid exits the turbine and enters the stator, which redirects the fluid at a favorable angle into the pump providing torque multiplication.

The change in angular momentum flux across each element produces a torque equal to the product of the local static pressure and radius integrated over the entire surface of each blade. An increase in element torque requires the pressure differential across a blade to increase proportionately. At some critical value of element torque, the pressure on the low pressure side of a blade drops

below the vapor pressure of the liquid, causing the nucleation of cavitation bubbles.

The effect of incipient cavitation is negligible on torque converter performance due to a minimal amount of liquid displaced by vapor in the toroidal flow circuit and confinement of bubbles to a relatively small region. Sustained operation at conditions of heavy cavitation alters converter performance due to larger vapor regions. Broadband noise that may become objectionable to vehicle occupants is produced by the collapse of cavitation bubbles as they travel to regions of higher pressure. Advanced stages of cavitation have been observed to cause a decrease in element torques that alters the characteristic relationship between speed and torque, see (Zeng 2002). This can be a problem for vehicle operation in that the converter no longer controls the engine speed as expected. Cavitation is suppressed by superimposing increased pressures upon the torque converter. The pressure imposed by the transmission control system is referred to as charge pressure, and is limited by the structural integrity of the torque converter housing and capacity of the transmission pump.

The purpose of parts I and II of the study is to quantify the effects of torque converter design parameters and operating conditions on cavitation through dimensional analysis of test results. The intention is to develop a tool for designing converters with minimal cavitation by fitting a power product model to the dimensionless data. In Part I, converters following strict rules of geometric similitude were analyzed. For Part II, the rules of similitude were relaxed to allow application of the dimensional analysis tool to a broader range of converter designs.

NOMENCLATURE

C_p	Specific heat	$kJ/kg \cdot K$
D	Diameter	m
K	K-factor	$RPM/Nm^{0.5}$
N_p	Pump Speed	RPM
Pr	Prandtl number	--
T_p	Pump Torque	Nm
$T_{s,i}$	Stator torque at onset of cavitation	Nm
U	Unit input speed	--
k	Thermal conductivity	$W/m \cdot K$
p_{ave}	Average pressure	Pa
p_b	Back pressure	Pa
p_c	Charge pressure	Pa
Δp	Pressure drop	Pa
ρ	Density	kg/m^3
μ	Viscosity	$N \cdot s/m^2$

GENERAL CONSIDERATIONS

Torque Converter Cavitation

The operating point most susceptible to the occurrence of cavitation in an automotive torque converter is stall, or zero turbine speed. Converter stall is produced in a vehicle by applying the brake and throttle simultaneously. This extends the instantaneous stall condition a vehicle undergoes when launching from a stopped position. Stall tests are useful for creating extreme conditions to study phenomena such as cavitation. Also, a vehicle can undergo sustained operation near stall when climbing a steep grade. The toroidal flow is highly three dimensional with high element flow incidence angles. The stator has previously been identified as the critical element in which incipient cavitation bubbles form as indicated by computational results of (Dong 2002 and Schweitzer 2003). Governed by hydrodynamic theory, pressures on the pressure surface of the stator blade are higher than the suction surface, with the greatest differential located at the leading edge of the blade. The incidence angle of flow into a stator at stall can be as high as 70 degrees for some designs, resulting in relatively large areas of flow separation and regions of low pressure on the suction surface of the blade. Experimentally these flow phenomena have been measured using dynamometer test setups by (By 1991 and Wantanabe 1996).

Fluctuating pressure measurements were made within the pump passage by (Zeng 2002) which recorded the pressure disturbances caused by the collapse of the cavitation bubbles as they traveled into regions of higher pressure within the pump. Mekkes et al. (2004), performed measurements of the fluctuating component of pressure at the leading edge of the stator, which showed the fluctuating pressure signal became damped as cavitation developed at the nose of the stator. The computational investigation performed by (Dong 2002) simulated the formation of cavitation bubbles within the toroidal flow circuit at stall. The results showed that at a particular pump speed, cavitation bubbles begin to develop at the leading edge of the stator. A subsequent increase in pump speed causes the pressure differential at the stator blade leading edge to increase. This produces an expansion of cavitation and greater displacement of liquid with vapor.

Acoustical Detection of Cavitation

Nearfield acoustical measurements were utilized to facilitate testing of multiple automotive torque converters without the need for specially instrumented converters. Similar measurement and post processing techniques were developed by (Kowalski 2005) to identify cavitation via the noise produced by the collapse of cavitation bubbles within the torque converter. It was observed from the sound measurements that a particular frequency characteristic correlated to the noise produced by the collapse of incipient cavitation bubbles. Cavitation related noise manifested itself in the frequency range of 6

to 20 kHz, the maximum measurable frequency. To remove noise not associated with cavitation a Kaiser Window high pass filter with a cutoff frequency of 6 kHz was applied to all acoustical measurements. Time averaging of filtered nearfield acoustical data at discrete, equally spaced pump speeds was performed to further enhance the ability to identify cavitation inception. Post processing the nearfield acoustical data in this manner revealed that an abrupt increase in filtered sound pressure level (SPL) occurred at a particular pump speed. This pump speed was identified as the onset of cavitation in this investigation. The specific procedure used to post process the data and identify the exact pump speed at the onset of cavitation is detailed by (Robinette 2007).

An example of a filtered SPL versus pump speed plot from this study is shown in Figure 2. At the transition to cavitating operation, an abrupt increase in filtered SPL is evident along with a drastic change in slope. Experimental investigations by (McNulty 1982 and Courbiere 1984) on centrifugal pumps have demonstrated the utility in acoustical measurements for detecting cavitation in turbomachinery. In both investigations, the cavitation threshold was noted by an abrupt increase in SPL as the turbomachine transitioned from a non-cavitating to cavitating operating regime. Consistent with these investigations, the first abrupt change in slope of the filtered SPL curve was recognized as the onset of cavitation.

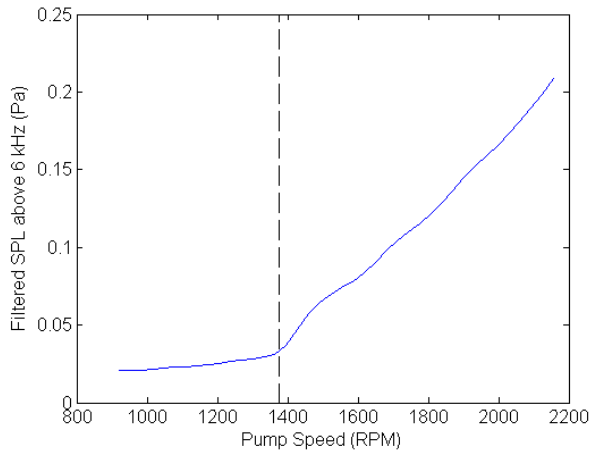

Figure 2. Filtered SPL versus pump speed for an automotive torque converter operating at stall, vertical dashed line indicates pump speed at onset of cavitation.

EXPERIMENTAL SETUP AND TEST PROCEDURE

Dynamometer Test Cell

A torque converter dynamometer test cell was constructed to acquire nearfield acoustical measurements for a variety of torque converter designs. The test cell consists of four major subsystems; dynamometers, a hydraulic supply system, acoustically treated test fixture and data acquisition systems, see Figure 3. A 213 kW direct current (DC) dynamometer was used to simulate engine speeds and torques at stall. A second DC dynamometer, used to simulate automatic transmission speeds and torques, was prevented from rotating to simulate stall operation. The hydraulic system allows setpoint control of the fluid pressures and temperature superimposed upon the torque converter to measure their impact on cavitation thresholds. A test fixture with acoustical treatment was necessary to create a near anechoic environment to accurately measure the cavitation noise produced within the torque converter. A minimum of 6 inches of acoustical treatment surrounded the torque converter, providing approximately 20 dB attenuation of standing waves and background noise. The configuration of torque converter, acoustical foam and nearfield microphone is depicted in Figure 4. Two data acquisition (DAQ) systems were used to acquire data during experimental testing. One DAQ system acquired nearfield acoustical data and pump speed at 51.2 kHz for determining the onset of cavitation. The other DAQ system acquired operational speeds, torques, pressures, temperatures and flows for use in dimensional analysis.

Figure 3. Torque converter dynamometer test cell, from left to right, hydraulic pump, input dynamometer, test fixture and output dynamometer.

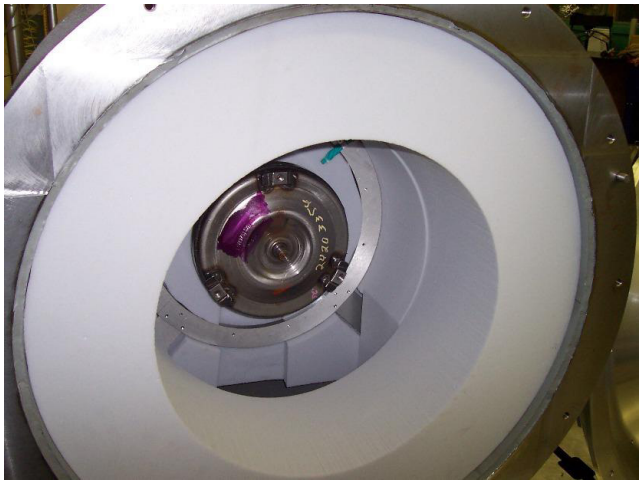

Figure 4. Torque converter, acoustical foam and nearfield microphone configuration in test fixture.

A standardized test procedure was developed to transition each torque converter from a non-cavitating to a cavitating condition. A series of stall speed sweep tests were completed to characterize cavitation thresholds for each torque converter at various combinations of pressures and input temperature. Each stall speed sweep test began at a pump speed of 500 RPM and increased at 40 RPM/s until the test was stopped at pump speeds above the onset of cavitation (~ 1200 to 2300 RPM). Fourteen stall speed sweeps were conducted for each design with charge pressure ranging from 483 to 896 kPa, back pressure from 276 to 827 kPa and input temperatures of 60, 70 and 80 °C.

Experimental Torque Converters

Two automotive torque converters were tested which maintained near exact geometric scaling. Every size dimension, such as thicknesses, torus profiles and clearances, were scaled by the ratio of the two converter diameters. Inlet and outlet blade angles were the same for both converters. Table 1 contains the design information for each element of the two torque converters tested. The only major difference between the small diameter, D_1, and large diameter, D_2, torque converters were the number of pump blades, 32 and 29, respectively. A difference in pump blade count was necessary to maintain identical performance metrics as discussed in the next section. The difference in blade count is not expected to cause a drastic departure from geometric similitude or to affect the analysis and conclusion of this investigation.

Table 1. Torque converter element design information

	D_1		D_2	
Element	Inlet/Outlet Angles	Blade Count	Inlet/Outlet Angles	Blade Count
Pump	-30°/+30°	32	-30°/+30°	29
Stator	+27°/+70°	17	+27°/+70°	17
Turbine	+61°/-63°	36	+61°/-63°	36

RESULTS AND DISCUSSION

Non-dimensionalizing the Onset of Cavitation

Analysis of test results from the similar converters was done to determine if cavitation threshold measurements can be manipulated into dimensionless parameters that include converter diameter. This would allow speed or torque thresholds determined experimentally for a given diameter, design and operating point to be scaled to multiple diameters when exact dimensional scaling and operating points are preserved.

Parameters commonly used to characterize torque converter performance are K-factor and unit input speed, U, shown in Equations 1 and 2:

$$K = \frac{N_p}{\sqrt{T_p}} \tag{1}$$

$$U = K\sqrt{\rho D^5} \tag{2}$$

K-factor is a semi-dimensionless parameter relating input torque and speed is used to compare performances of converters with constant diameter and constant fluid properties. Test results can be scaled to other diameters using the dimensionless version of K-factor, unit input speed, U, which incorporates terms for diameter and fluid density. The inverse square of unit input speed is a more common presentation of the dimensionless turbomachinery parameter known as the torque capacity coefficient. The two converters used in this study have different values for K-factor but the same U because of their similar torus shape and blade angles. During stall operation, U for similar converter designs remains fixed, so it is not suitable for scaling onset of cavitation thresholds. A new dimensionless parameter must be developed.

Due to the relationship between speed and torque, either could be used to describe critical operating thresholds at the onset of cavitation. Torque was selected since torque capacity is an important factor when matching a converter to a particular engine. Further, stator torque at the onset of cavitation, $T_{s,i}$, was selected over pump torque for comparing different converter designs since it has been shown that cavitation usually starts in the stator, see (Robinette 2007). In general, small diameter torque converters will have higher pump speeds, but lower torque thresholds at the onset of cavitation than larger diameter units of similar element designs. This is readily seen in the plots of filtered SPL versus pump speed (left) and stator torque (right) in Figure 5. Figure 6 is a plot of $T_{s,i}$ versus charge pressure for all fourteen operating conditions. The stator torque cavitation threshold is greater for the larger diameter torque converter by 95 to 118 Nm with 95% confidence.

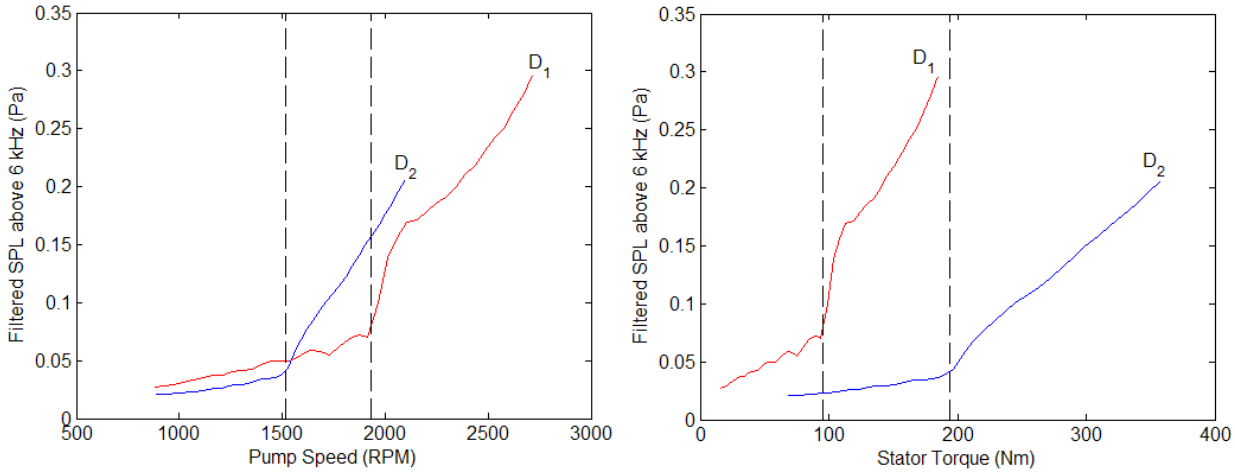

Figure 5. Filtered SPL versus pump speed (left) and stator torque (right) for stall speed sweep of 40 RPM/s at p_c = 791 kPa, p_b = 584 kPa and θ_{in} = 70 °C. Vertical dashed lines indicate onset of cavitation.

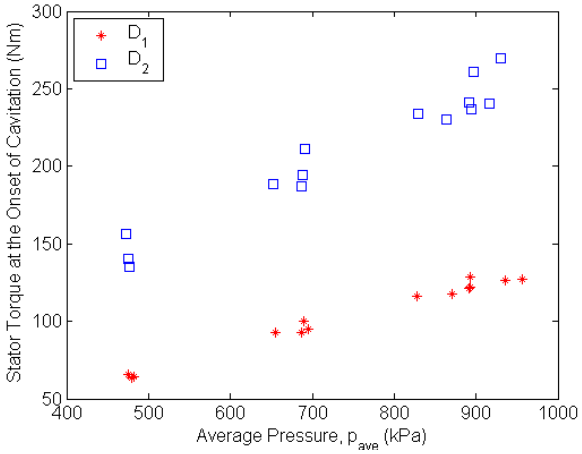

Figure 6. Stator torque at the onset of cavitation threshold versus average absolute pressure superimposed upon the torque converter.

Stator torque at incipient cavitation is a function of those variables that determine the boundary value problem of the toroidal flow, primarily the size and shape of the torque converter, blade geometries, and the charge pressure, p_c, and back pressure, p_b, superimposed upon the unit. Charge and back pressures can be transformed into average pressure, p_{ave}, and pressure drop, Δp, which are more suitable for the dimensional analysis. Secondary variables include cooling through-flow rate, Q, and the relevant mean fluid properties at a representative temperature. Through-flow cooling is a function of the controlled operating points of charge pressure and pressure drop across the unit, and was not explicitly included in the list of variables that affect stator torque at the onset of cavitation. Equation 3 represents $T_{s,i}$ as a function of both the primary and secondary variables, with all temperature dependent fluid properties determined at the input temperature of the cooling flow supplied to the torque converter:

$$T_{s,i} = f\left(D, p_{ave}, \Delta p, \rho, \mu, C_p, k\right) \tag{3}$$

The dimensionless form of Equation 3 can be resolved into a function of two dimensionless operating point parameters using the repeating variables of D, ρ, p_{ave} and C_p. The result, Equation 4, is a dimensionless quantity relating $T_{s,i}$ to size of the torque converter and average pressure superimposed upon the unit and will be referred to as dimensionless stator torque. This quantity is then a function of two dimensionless operating point parameters, dimensionless operating pressure and the Prandtl number:

$$\frac{T_{s,i}}{D^3 p_{ave}} = f\left(\frac{\Delta p}{p_{ave}}, \mathrm{Pr}\right) \tag{4}$$

Dimensionless stator torque represents a similarity condition when geometric similitude is observed. Thus, the stator torque cavitation threshold for a particular stall operating point can be scaled to other diameters. The similarity condition for dimensionless stator torque is expressed in Equation 5. The subscript 1 represents the known cavitation threshold and diameter, while subscript 2 represents the cavitation threshold and diameter that are to be scaled. Figure 7 illustrates this point more clearly for the converters tested in this investigation. The onset of cavitation in Figure 7 is indicated by the vertical dashed lines, which differ by 1.69%. This observation was found to be valid for all fourteen stall operating points tested:

$$\left(\frac{T_{s,i}}{D^3 p_{ave}}\right)_1 = \left(\frac{T_{s,i}}{D^3 p_{ave}}\right)_2 \tag{5}$$

It should be noted that p_{ave} in Equation 5 must be equivalent, i.e. same combination of charge and back pressures, to properly scale $T_{s,i}$ from one diameter to another. The ratio of average pressures for each diameter

simply becomes unity, and can be subsequently dropped from Equation 5.

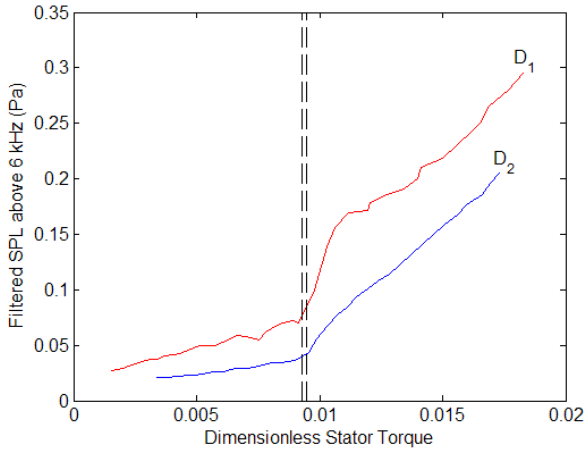

Figure 7. Filtered SPL versus dimensionless stator torque for stall speed sweep of 40 RPM/s at p_c = 791 kPa, p_b = 584 kPa and θ_{in} = 70 °C. Vertical dashed lines indicate onset of cavitation.

Power Product Model

At stall, K-factor (Equation 1) is a constant value for a given design so long as heavy and sustained cavitation does not disrupt normal toroidal flow conditions. For a particular operating point, the onset of cavitation will occur at some pump speed and corresponding value of pump torque and lay on the K-factor curve for a given design. Figure 8 contains all $T_{s,i}$ versus $N_{p,i}$ data, indirectly demonstrating the K-factor relationship for either diameter, since stator torque can be determined from pump and turbine torques. The results of Figure 8, however, are not readily applicable to other diameter converters. A power product model (Equation 6) was fit to dimensionless stator torque values at the onset of cavitation for the range of stall operating points tested, as noted in Table 2, to determine the functional relationship for Equation 4 and develop a predictive tool:

$$\frac{T_{s,i}}{D^3 p_{ave}} = 0.006\left[\left(\frac{\Delta p}{p_{ave}}\right)^{0.042} \mathrm{Pr}^{0.11}\right] \quad (6)$$

For Equation 6, dimensionless stator torque is the response variable and the dimensionless quantities of operating pressures and Prandtl number are the dimensionless regressors. The coefficients and exponents of Equation 6 were determined using a nonlinear least squares fit using a Gaussian Newton numerical approximation technique. The power product model shown in Figure 9 had a computed percent root mean square error *(%RMSE)* of 3.7%:

$$\%RMSE = \sqrt{\frac{\sum_{i=1}^{n}\left(\frac{y_i - \hat{y}_i}{y_i} * 100\right)^2}{n-p}} \quad (7)$$

From studentized residual and leverage rule statistical tests, see (Kutner 2004), it was determined that the power product model did not contain outliers.

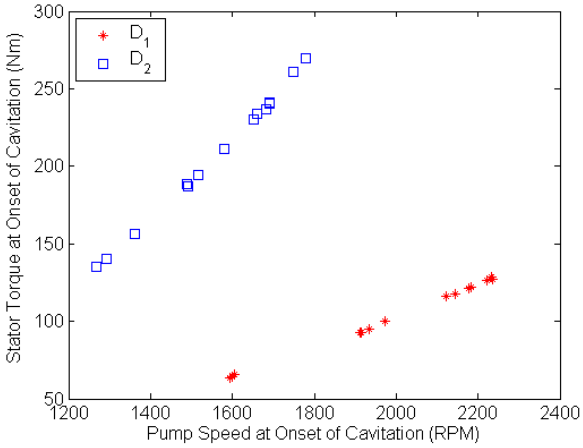

Figure 8. Stator torque at the onset of cavitation plotted against pump speed at the onset of cavitation over all stall operating points.

Table 2. Range of operating point parameters tested

Operating Point	Low	High
Average Pressure	481 kPa	963 kPa
Pressure Drop	69 kPa	345 kPa
Input Temperature	60 °C	80 °C

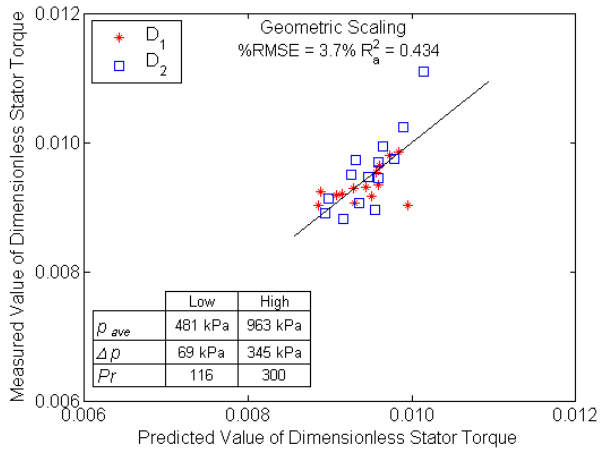

Figure 9. Dimensionless power product model fit on dimensionless stator torque for torque converters of exact geometric scaling, over range of operating points in Table 2.

Model goodness of fit was checked by computing the adjusted coefficient of multiple determination, R^2_a, using Equation 8. The value of R^2_a can be interpreted as the proportionate reduction in the variation in the response given the set of regressors in the model:

$$R_a^2 = 1 - \frac{\sum_{i=1}^{n}(y_i - \hat{y}_i)^2 \Big/ n-p}{\sum_{i=1}^{n}(y_i - \bar{y})^2 \Big/ n-1} \quad (8)$$

The computed value was relatively low, at 0.434, compared to values of around 0.85 that are typical of good fit models. The low R^2_a value indicates that the model and regressors did not account for approximately 60 % of the variation in dimensionless stator torque. This is caused mainly by a limited linear association between the dimensionless response and model parameters. More specifically, a multitude of least squares solutions exists in terms of estimated slopes and exponents. Thus, a variety of least squared determined power product models may be fit to the data set resulting in the same overall minimized error. However, the low value R^2_a does not detract from the predictive capability of the model, but its overall utility is minimal as predictions are limited to scaling cavitation thresholds for a single set of element designs and torus dimensions.

Use of dimensionless stator torque results in a nearly constant term for incipient cavitation over the range of operating points tested for a given diameter converter. It can be noted from Figure 10, a plot of mean and predicted values for each diameter that there is little variation between either diameter for all average pressures (Figure 10a) and input temperatures (Figure 10b) tested. Dimensionless stator torque does not vary greatly with average pressure (Figure 10a), a consequence of non-dimensionalizing stator torque by average pressure. Some degree of variation with input temperature is evident (Figure 10b), as it is not used explicitly or implicitly through fluid properties to non-dimensionalize stator torque at the onset of cavitation. The small variation in dimensionless stator torque does not particularly lend itself to empirical modeling. The results are not surprising since designs with near exact geometric similitude have identical dimensionless quantities that characterize their design, causing potential regressor terms to fall out of the power product model equation. For an adequate model to be developed the variation in dimensionless stator torque would have to be increased by including test results from converters that do not follow exact geometric similitude, but are defined by ranges of design parameters. Additional testing and analysis were completed and are detailed in Part II of the paper. Results demonstrated a stronger linear association between dimensionless response and regressors and increased value of R^2_a.

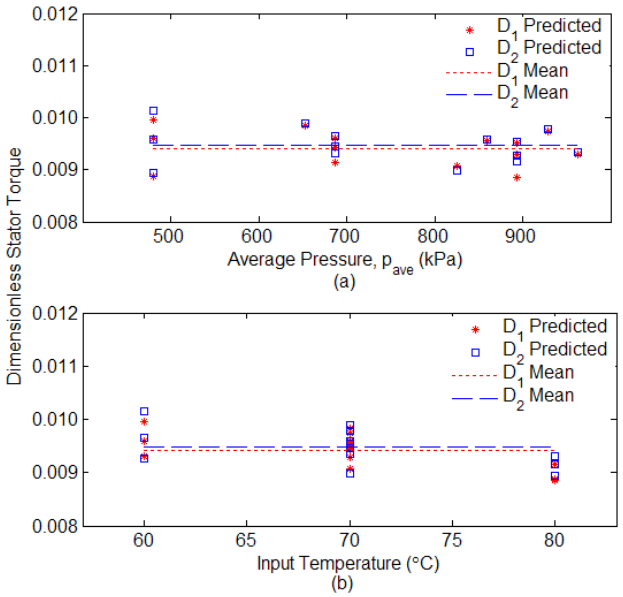

Figure 10. Predicted value and mean measured value of dimensionless stator torque as a function of average pressure (a) and input temperature (b) from PP model.

CONCLUSIONS

Dimensional analysis was applied to experimentally obtained stall operating thresholds at the onset of cavitation for two torque converters of exact geometric scaling. Stator torque was determined to be the preferred operating threshold parameter at cavitation as it properly conveys the torque capacity for a given design and is most closely associated with the cavitation phenomenon. A scalable term for dimensionless stator torque was developed by relating cavitation threshold stator torque to the size of the torque converter and average pressure applied to the unit. Further, a power product model based upon dimensionless stator torque was developed for the range of operating points tested, resulting in a *%RMSE* of 3.7% and R^2_a of 0.434. The low value of R^2_a computed for the model indicates difficulties performing a least squares regression on a data set of limited variation in response and regressor variables. The shortcomings associated with the power product model and using converters only of geometric similitude will be addressed in Part II of this two part paper, along with development of a more generalized model for predicting $T_{s,i}$, applicable to three element torque converter designs with relaxed geometric similitude.

REFERENCES

1. By, R., Lakshiminarayana, B., "Static Pressure Measurements in a Torque Converter Stator," SAE 911924, 1991.

2. Courbiere, P., "An Acoustical Method for Characterizing the Onset of Cavitation in Nozzles and Pumps," 2nd International Symposium on Cavitation Inception, ASME Winter Meeting, New Orleans, 1984.

3. Dong, Y., Korivi, V., Attibele, P., and Yuan, Y., ”Torque Converter CFD Engineering Part II: Performance Improvement through Core Leakage Flow and Cavitation Control,” SAE 2002-01-0884, 2002.

4. Kowalski, D., Anderson, C., Blough, J., “Cavitation Detection in Automotive Torque Converters using Nearfield Acoustical Measurements,” SAE 2005-01-2516, 2005.

5. Kutner, M. H., Nachtsheim, C. J., Neter, J., *Applied Linear Regression Models*, 4th Edition McGraw Hill, 2004.

6. McNulty, P. J., Pearsall, I. S., “Cavitation Inception in Pumps,” ASME J. Fluids Eng., Vol. 104, pp. 99-104, 1982.

7. Mekkes, J., Anderson, C., Narain, A., “Static Pressure Measurements on the Nose of a Torque Converter Stator during Cavitation,” 10th ISROMAC, 2004.

8. Robinette, D., Anderson, C., Blough J., Johnson, M., Maddock, D., and Schweitzer, J., “Characterizing the Effect of Torque Converter Design Parameters on the Onset of Cavitation at Stall,” SAE Noise and Vibration Conference, Chicago, IL, 2007-01-2231, 2007.

9. Schweitzer, J., Gandham, J., “Computational Fluid Dynamics in Torque Converters: Validation and Application,” International J. of Rotating Machinery, Vol. 9, pp. 411-418, 2003.

10. Wantanabe, H., Yoshida, K., Yamada, M., and Kojima, M., “Flow Visualization and Measurement in the Stator of a Torque Converter,” JSAE Review, Vol. 17, pp. 25-30, 1996.

11. Zeng, L., Anderson, C., Sweger, P. O., Narain, A., ”Experimental Investigation of Cavitation Signatures in an Automotive Torque Converter using a Microwave Telemetry Technique,” 9th ISORMAC, 2002.